

Elastic and Inelastic Evanescent-Wave Mirrors for Cold Atoms

D. Voigt, B.T. Wolschrijn, R.A. Cornelussen, R. Jansen, N. Bhattacharya,
H.B. van Linden van den Heuvell, and R.J.C. Spreeuw
*Van der Waals-Zeeman Institute, University of Amsterdam,
Valckenierstraat 65, 1018 XE Amsterdam, the Netherlands*
<http://www.science.uva.nl/research/aplp/>
(October 24, 2018)

We report on experiments on an evanescent-wave mirror for cold ^{87}Rb atoms. Measurements of the bouncing fraction show the importance of the Van der Waals attraction to the surface. We have directly observed radiation pressure parallel to the surface, exerted on the atoms by the evanescent-wave mirror. We analyze the radiation pressure by imaging the motion of the atom cloud after the bounce. The number of photon recoils ranges from 2 to 31. This is independent of laser power, inversely proportional to the detuning and proportional to the evanescent-wave decay length. By operating the mirror on an open transition, we have also observed atoms that bounce inelastically due to a spontaneous Raman transition. The observed distributions consist of a dense peak at the minimum velocity and a long tail of faster atoms, showing that the transition is a stochastic process with a strong preference to occur near the turning point of the bounce.

32.80.Lg, 42.50.Vk, 03.75.-b

I. INTRODUCTION

The use of evanescent waves (EW) as a tool to manipulate the motion of neutral atoms has been proposed by Cook and Hill [1]. Since then, EW mirrors have become an important tool in atom optics [2]. They have been demonstrated for atomic beams at grazing incidence [3] and for ultracold atoms at normal incidence [4]. In many experiments the scattering of EW photons was undesirable because it makes the mirror incoherent.

However, an EW mirror is also a promising tool for efficient loading of low-dimensional optical atom traps in the vicinity of the dielectric surface [5–8]. In these schemes, spontaneous optical transitions play a crucial role in providing dissipation [9–11]. Since inelastic bouncing may increase the atomic phase-space density, this may open a route towards quantum degenerate gases, which does not use evaporative cooling. Thus one may hope to achieve “atom lasers” [12] which are open, driven systems out of thermal equilibrium, similar to optical lasers [13]. It is this application of EW mirrors which drives our interest in experimental control of the photon scattering of bouncing atoms.

In a first experiment involving the scattering of evanescent photons we have observed directly for the first time the radiation pressure exerted by evanescent waves on

cold atoms [14]. In a second experiment we directly observe clouds of atoms which bounce inelastically by changing their hyperfine ground state.

II. EXPERIMENTAL SETUP

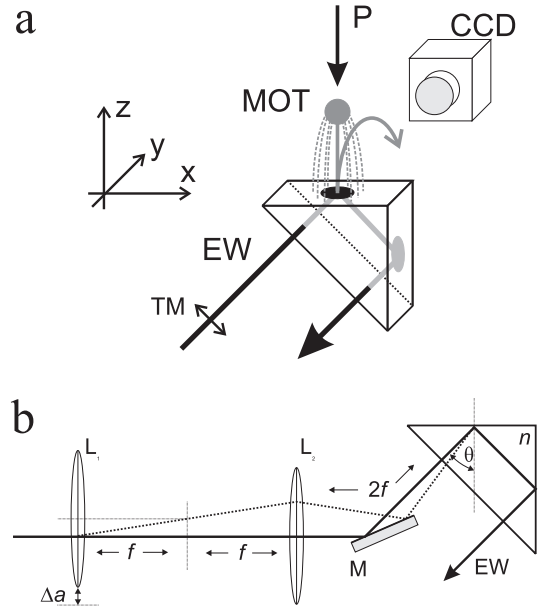


FIG. 1. Experimental setup. (a) Cold ^{87}Rb atoms (MOT), are released 6.6 mm above a right-angle prism. An evanescent wave is created by beam EW. Fluorescence from probe beam P is imaged onto a CCD camera. (b) Confocal relay telescope for adjusting the angle of incidence θ . The lenses $L_{1,2}$ have equal focal length, $f = 75$ mm. A translation of L_1 by a distance Δa changes the angle of incidence by $\Delta\theta = \Delta a/fn$. The position of the EW spot remains fixed. M is a mirror.

Our experiments are performed in a vapor cell. Approximately 10^7 atoms of ^{87}Rb are loaded out of the background vapor into a magneto-optical trap (MOT) and are subsequently cooled to $10\ \mu\text{K}$ using polarization gradient cooling (optical molasses). The cold atom cloud is released in the $F = 2$ ground state. After a free fall of 6.6 mm the atoms reach the horizontal surface of a right-angle BK7 prism (refractive index $n = 1.51$), see Fig. 1(a).

The EW beam emerges from a single-mode optical

fiber, is collimated and directed into the prism through a relay telescope, see Fig. 1(b). The angle of incidence θ is controlled by the vertical displacement Δa of the first lens L_1 . The second lens L_2 images the beam to a *fixed* spot at the prism surface. A displacement Δa changes the angle by $\Delta\theta = \Delta a/nf$. The beam has a minimum waist of $335\text{ }\mu\text{m}$ at the surface ($1/e^2$ intensity radius) and a nearly diffraction limited divergence half-angle of $< 1\text{ mrad}$.

For the EW, an injection-locked single mode laser diode provides up to 28 mW of optical power behind the fiber. It is seeded by an external grating stabilized diode laser, locked to the ^{87}Rb hyperfine transition $5S_{1/2}(F=2) \rightarrow 5P_{3/2}(F'=3)$ of the D_2 line. The detuning with respect to this transition determines the optical potential for atoms released from the MOT in the $F=2$ ground state.

III. VAN DER WAALS SURFACE ATTRACTION

The EW field is $E(\mathbf{r}) \propto \exp(ik_x x) \exp(-\kappa z)$, with $k_x = k_0 n \sin\theta$ and $\kappa = k_0 \sqrt{n^2 \sin^2\theta - 1}$, where $k_0 = 2\pi/\lambda_0$ is the vacuum wave number. The optical dipole potential for a two-level atom can be written as $\mathcal{U}_{\text{dip}}(z) = \mathcal{U}_0 \exp(-2\kappa z)$. In the limit of large detuning, $|\delta| \gg \Gamma$, and low saturation, $s_0 \ll 1$, the maximum potential at the surface is $\mathcal{U}_0 = \hbar\delta s_0/2$, with a saturation parameter $s_0 \simeq (\Gamma/2\delta)^2 TI/I_0$ [15]. Here I is the intensity of the incident beam inside the prism, $I_0 = 1.65\text{ mW/cm}^2$ is the saturation intensity for rubidium and $\Gamma = 2\pi \times 6.0\text{ MHz}$ is the natural linewidth. The factor T ranges from 5.4 – 6.0 (2.5 – 2.65) for a TM (TE) polarized EW [16]. The detuning of the laser frequency ω_L with respect to the atomic transition frequency ω_0 is defined as $\delta = \omega_L - \omega_0$. Thus a “blue” detuning ($\delta > 0$) yields an exponential potential barrier for incoming atoms. A classical turning point exists if the barrier height exceeds the kinetic energy $p_i^2/2M$ of an incident atom.

In reality, the barrier height is determined not only by the dipole potential. The attractive Van der Waals potential near the surface,

$$\mathcal{U}_{\text{vdW}}(z) = -\frac{3(n^2 - 1)}{16(n^2 + 1)} \frac{\hbar\Gamma}{(k_0 z)^3}. \quad (1)$$

lowers the maximum potential and thus decreases the surface area on which atoms can bounce [17]. Gravity can usually be neglected on the length scale of the EW decay length.

We have measured the fraction of bouncing atoms using a weak resonant probe beam, inserted between the MOT position and the surface. Time-of-flight signals were recorded on a photodiode and the integrated absorption signal was measured for both falling and bouncing atoms. The extracted fractions of bouncing atoms are shown in Fig. 2, as a function of the strength of the optical potential \mathcal{U}_0 . The logarithmic dependence is a

consequence of the gaussian beam profile of the EW. Also shown are two calculations of the bouncing fraction using no adjustable parameters, (i) assuming a purely optical potential (dashed line), and (ii) taking into account also the Van der Waals surface attraction (solid line). The latter clearly yields much better agreement. Similar measurements have previously been performed by Landragin *et al.* [17].

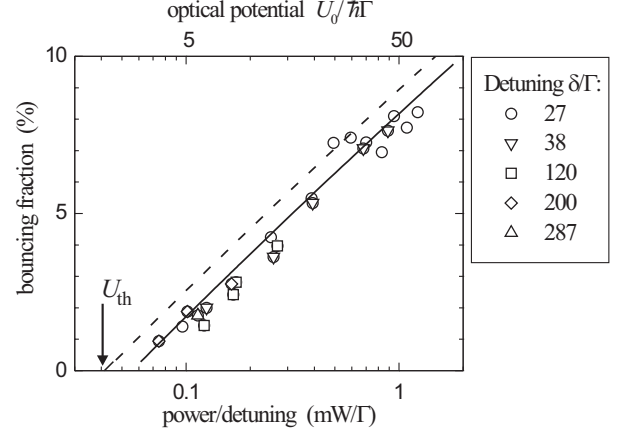


FIG. 2. Bouncing fraction vs. evanescent-wave power and detuning: TE-polarisation, power between 0–28 mW, detuning in units of $\Gamma = 2\pi \times 6\text{ MHz}$, angle $\theta = \theta_c + 8.7\text{ mrad}$, laser waist $w_0 = 335\text{ }\mu\text{m}$. Predictions with (solid line) and without (dashed) Van der Waals interaction. The (optical) threshold potential is indicated by an arrow.

IV. RADIATION PRESSURE BY EVANESCENT WAVES

The evanescent wavevector $\mathbf{k} = (k_x, 0, i\kappa)$ contains a real (propagating) component along the surface. It has been predicted already by Roosen and Imbert [18] that therefore an evanescent wave should exert radiation pressure parallel to the surface. A similar scattering force has been observed for micrometer-sized dielectric spheres [19]. The photon scattering rate of a two-level atom in steady state at low saturation is $\Gamma' \approx s\Gamma/2 = (\Gamma/\hbar\delta)\mathcal{U}_{\text{dip}}$ [15]. An atom bouncing on an EW mirror sees a time dependent saturation parameter $s(t)$. Assuming that the excited state population follows adiabatically, we can integrate the scattering rate along an atom’s trajectory to get the number of scattered photons, $N_{\text{scat}} = \int \Gamma'(t)dt$. For a purely optical potential this leads to an analytical solution:

$$N_{\text{scat}} = \frac{\Gamma}{\delta} \frac{p_i}{\hbar\kappa}. \quad (2)$$

Note that N_{scat} is independent of \mathcal{U}_0 , as a consequence of the exponential shape of the potential.

We have observed this evanescent-wave radiation pressure directly by imaging the bouncing atom clouds [14]. The fluorescence induced by a 0.5 ms pulse of resonant

probe light was imaged onto a digital frame-transfer CCD camera. A repumping beam, tuned to the $F = 1 \rightarrow F' = 2$ transition of the D_1 line (795 nm), was used to counteract optical pumping to the $F = 1$ ground state by the probe.

We measure the trajectories of bouncing atoms by taking a sequence of images with incremental time delays. A typical series with increments of 10 ms is shown in Fig. 3. A new sample was prepared for each shot; each image was averaged over 10 shots. In the lower half of the Figure we see the atom cloud bouncing up slightly sideways.

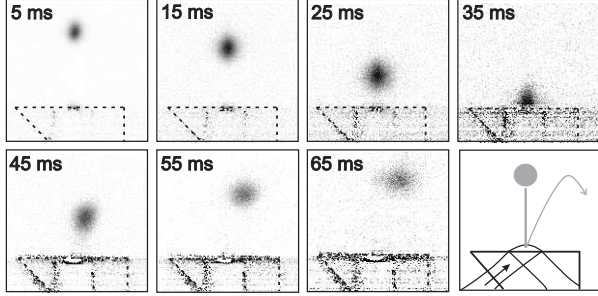


FIG. 3. Fluorescence images of a bouncing atom cloud. The first image was taken 5 ms after releasing the atoms from the MOT. The configuration of prism and evanescent wave is illustrated by the schematic (Field of view: $10.2 \times 10.2 \text{ mm}^2$).

The horizontal velocity change during the bounce is extracted from a sequence of images. In Fig. 4, we show how this velocity kick depends on the laser detuning δ and on the EW decay length $\xi \equiv 1/\kappa(\theta)$, by varying the angle θ . The velocity kick has been expressed in units of the EW photon recoil, $p_{\text{rec}} = \hbar k_0 n \sin \theta$, with $\hbar k_0/M = 5.88 \text{ mm/s}$. In Fig. 4(a), the detuning is varied from 188 – 1400 MHz (31 – 233 Γ). Two sets of data are shown, taken for two different EW decay lengths $\xi = 2.8 \text{ }\mu\text{m}$ and $0.67 \text{ }\mu\text{m}$. We find that $N_{\text{scat}} \propto \delta^{-1}$, as expected. The predictions based on Eq. (2) are indicated in the figure (solid lines).

In Fig. 4(b), the detuning was kept fixed at 44 Γ and the angle of incidence varied from 0.9 – 24.0 mrad above the critical angle. This leads to a variation of decay length ξ from 2.8 – 0.53 μm . Here also, we find a linear dependence on ξ . Clearly, a steep optical potential, i.e. a small decay length, causes less radiation pressure than a shallow potential. A linear fit to the data for $\xi < 1 \text{ }\mu\text{m}$, extrapolates to an offset of approximately 3 photon recoils in the limit $\xi \rightarrow 0$ [thin solid line in Fig. 4(b)]. We attribute this offset to diffusely scattered EW light due to roughness of the prism surface which propagates into the vacuum. Preferential light scattering in the direction of the EW propagation can be explained if the power spectrum of the surface roughness is narrow compared to $1/\lambda$ [20]. The effect of surface roughness has previously been observed as a broadening of bouncing atom clouds by the roughness of the *dipole potential* [21]. In our case, we

observe a change in center of mass motion of the clouds due to an increase in the *spontaneous scattering force*. Such a contribution to the radiation pressure due to surface roughness vanishes in the limit of large detuning δ . Thus, we find no significant offset in Fig. 4(a).

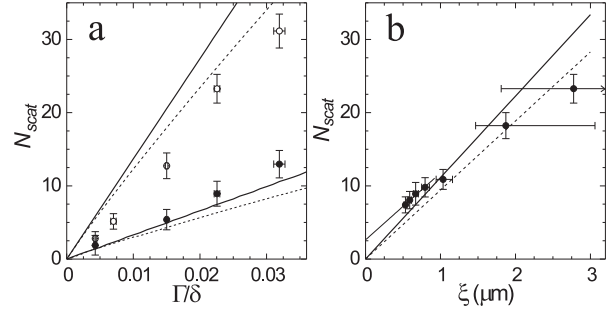


FIG. 4. Radiation pressure on bouncing atoms expressed as number of absorbed photons, N_{scat} . (a) Detuning δ varied for $\xi = 2.8 \text{ }\mu\text{m}$ (open points) and $0.67 \text{ }\mu\text{m}$ (solid points). (b) EW decay length ξ varied for $\delta = 44 \text{ }\Gamma$. The laser power was 19 mW. The thin solid line is a linear fit through the first four data points. Theoretical predictions: two-level atom (see Eq. (2), thick solid lines). Excited-state hyperfine structure and saturation taken into account (dashed lines).

We have also verified that there is no significant dependence on the power of the EW, in accordance with Eq. (2). Only a slight increase with EW power is observed, which may again be due to diffusely scattered light. The optical power mainly determines the effective mirror surface and thus the fraction of bouncing atoms. This is also visible in the horizontal width of bouncing clouds.

We find a significant correction due to the excited state manifold $F' = \{0, 1, 2, 3\}$ of ^{87}Rb . Besides $F' = 3$, also $F' = 1, 2$ contribute to the mirror potential, whereas they do not much affect the scattering rate. For an EW detuning of 44 Γ , this reduces the number of scattered photons by typically 9% compared to a two-level atom, when we average over the contributions from different magnetic sublevels (dashed lines).

V. INELASTIC BOUNCING

If the mirror laser is tuned to an open transition, photon scattering can lead to a spontaneous Raman transition to the other hyperfine ground state. The atom will then leave the surface on a different potential curve from when it approached the surface. Hence, the kinetic energy after the bounce will in general be different from that before the bounce.

We performed experiments where the EW laser was tuned in the blue wing of the $F = 1 \rightarrow F' = 2$ transition of the D_2 line of ^{87}Rb , with a detuning $\delta_1 \ll \delta_{\text{GHF}}$, with

$\delta_{\text{GHF}} = 2\pi \times 6.8$ GHz the ground state hyperfine splitting. Atoms in $F = 2$ see the EW mirror with a detuning which is larger by a factor of approximately $\delta_2/\delta_1 \approx \delta_{\text{GHF}}/\delta_1$ and therefore see a much weaker potential. Thus they leave the surface with a reduced kinetic energy. Repeating this procedure leads to so-called “evanescent-wave cooling” [9–11].

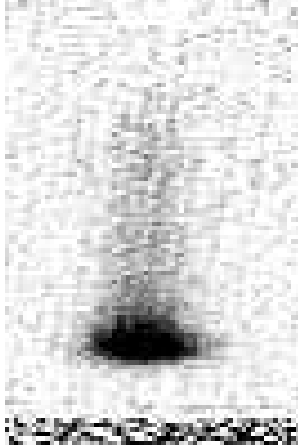


FIG. 5. Absorption image of atoms bouncing inelastically from an evanescent-wave mirror. The image was taken 14 ms after the bounce. The field of view is 3.4×5.1 mm².

We observe the inelastically bouncing atoms directly by imaging the absorption of a weak resonant probe pulse onto a digital CCD camera. In Fig. 5 we show a typical image, taken when the slowest atoms have reached their upper turning point. The observed clouds are highly asymmetric, with a dense peak at the lower edge of the cloud and a tail of faster atoms extending upward. The dense peak contains the atoms that made the Raman transition near the turning point, because here they move slowly in a relatively high light intensity. The tail contains faster atoms, which have made the Raman transition while falling down to, or bouncing up from the surface. The density distribution in the vertical direction agrees well with a calculation where the atoms are modeled as point particles moving on an exponential potential curve.

VI. OUTLOOK

The result of the inelastic bouncing experiment shows the preference for making a spontaneous Raman transition near the turning point of the bounce. This is of great importance for our ongoing experiments which are aimed at trapping the cold atoms near the turning point, in a low-dimensional optical trap. Although the present experiment showed a relatively high density at the lowest possible bouncing velocity, it is unlikely that the phase-space density has been increased. It remains to be inves-

tigated under what conditions such an increase can be obtained and by how much.

The scattering of evanescent photons is an essential ingredient in our experiment toward loading low-dimensional optical traps. At the same time, once loaded into the trap, we wish the atoms to scatter at a very low rate. In order to meet these conflicting requirements our present experiments are aimed at trapping the atoms in a so-called dark state which no longer interacts with the evanescent wave. This requires the use of circularly polarized evanescent waves. This procedure should lead to an ultracold low-dimensional gas and may ultimately yield an all-optical road to quantum-degeneracy and an atom laser.

ACKNOWLEDGMENTS

We thank E.C. Schilder for help with the experiments. This work is part of the research program of the “Stichting voor Fundamenteel Onderzoek der Materie (FOM)” which is financially supported by the “Nederlandse Organisatie voor Wetenschappelijk Onderzoek (NWO)”. R.S. has been financially supported by the Royal Netherlands Academy of Arts and Sciences.

-
- [1] R. J. Cook and R. K. Hill, *Opt. Commun.* **43**, 258 (1982).
 - [2] C. Adams, M. Sigel, and J. Mlynek, *Phys. Reports* **240**, 143 (1994).
 - [3] V.I. Balykin, V.S. Letokhov, Yu.B. Ovchinnikov, and A.I. Sidorov, *JETP Lett.* **45**, 353 (1987).
 - [4] M. Kasevich, D. Weiss, and S. Chu, *Opt. Lett.* **15**, 607 (1990).
 - [5] P. Desbiolles and J. Dalibard, *Opt. Commun.* **132**, 540 (1996).
 - [6] W. Power, T. Pfau, and M. Wilkens, *Opt. Commun.* **143**, 125 (1997).
 - [7] H. Gauck *et al.*, *Phys. Rev. Lett.* **81**, 5298 (1998).
 - [8] R. J. C. Spreeuw, D. Voigt, B. T. Wolschrijn, and H. B. van Linden van den Heuvell, *Phys. Rev. A* **61**, 053604 (2000).
 - [9] P. Desbiolles, M. Arndt, P. Szriftgiser, and J. Dalibard, *Phys. Rev. A* **54**, 4294 (1996).
 - [10] Y. B. Ovchinnikov, I. Manek, and R. Grimm, *Phys. Rev. Lett.* **79**, 2225 (1997).
 - [11] D. Laryushin, Y. B. Ovchinnikov, V. Balykin, and V. Letokhov, *Opt. Commun.* **135**, 138 (1997).
 - [12] M.-O. Mewes *et al.*, *Phys. Rev. Lett.* **78**, 582 (1997); B.P. Anderson and M.A. Kasevich, *Science* **282**, 1686 (1998); E. Hagley *et al.*, *Science* **283**, 1706 (1999); I. Bloch, T.W. Hänsch, and T. Esslinger, *Phys. Rev. Lett.* **82**, 3008 (1999).
 - [13] R. Spreeuw, T. Pfau, U. Janicke, and M. Wilkens, *Europhys. Lett.* **32**, 469 (1995).

- [14] D. Voigt *et al.*, Phys. Rev. A **61**, 063412 (2000).
- [15] C. Cohen-Tannoudji, J. Dupont-Roc, and G. Grynberg, *Atom-photon interactions* (Wiley, New York, 1992).
- [16] The “transmissivity” into the evanescent wave follows from the Fresnel coefficients, $T_{\text{TM}} = 4n \cos^2 \theta (2n^2 \sin^2 \theta - 1) / (\cos^2 \theta + n^2(n^2 \sin^2 \theta - 1))$ and $T_{\text{TE}} = 4n \cos^2 \theta / (n^2 - 1)$.
- [17] A. Landragin *et al.*, Phys. Rev. Lett. **77**, 1464 (1996).
- [18] G. Roosen and C. Imbert, Opt. Commun. **18**, 247 (1976).
- [19] S. Kawata and T. Sugiura, Opt. Lett. **17**, 772 (1992).
- [20] C. Henkel *et al.*, Phys. Rev. A **55**, 1160 (1997).
- [21] A. Landragin *et al.*, Opt. Lett. **21**, 1591 (1996).